Simple technique for bulk quantity synthesis of ZnO tetrapod nanorods

V. A. L. Roy,[1] A. B. Djurišić[1,2], Q. Li,[2] S. J. Xu,[2] H. F. Lui,[3] C. Surya,[3] and J. Gao[2]
[1]*Department of Electrical & Electronic Engineering, University of Hong Kong, Pokfulam Road, Hong Kong*
[2]*Department of Physics, University of Hong Kong, Pokfulam Road, Hong Kong*
[3] *Department of Electronic and Information Engineering, Hong Kong Polytechnic University, Hung Hom, Kowloon, Hong Kong*

In this work, we report a simple method for mass production of ZnO tetrapod nanorods. A mixture of Zn and graphite powders (ratio 2:1) was placed in a quartz tube. The quartz tube was placed in a horizontal tube furnace and heated up to 950°C. The tube was then removed from the furnace and quenched to room temperature. Fluffy products white in color were formed on the walls of the tube. Obtained products were characterized by X-ray diffraction, scanning electron microscopy (SEM), transmission electron microscopy (TEM) and photoluminescence. SEM images showed tetrapod-like ZnO nanorods. The four tetrapod legs were approximately equal length, and the length of tetrapod legs was in the range ~1-3 μm. We investigated influence of the growth temperature (in the range from 700°C to 1100°C) and Zn to catalyst ratio to the properties of obtained products. Fabrication in different atmospheres (air, argon, nitrogen, humid argon, and humid nitrogen) was also performed. The influence of growth conditions (temperature, atmosphere, and catalyst concentration) to the formation and properties of ZnO nanorods is discussed.

Keywords: ZnO nanorods, SEM, photoluminescence

1. INTRODUCTION

Semiconductor nanostructures are of considerable interest for the study of their exceptional electronic and optical properties, as well as potential for applications in nanostructure-based devices. As a wide band gap semiconductor with large exciton binding energy, ZnO is of lots of interest for optoelectronic devices. Different fabrication methods have been reported for ZnO nanoparticles,[1,2] and one dimensional nanostructures.[3-13] Different shapes of one dimensional nanostructures were reported (tetrapod nanorods, nanowires, or nanobelts). ZnO nanobelts were fabricated by evaporation of ZnO powder at high temperature[3] and thermal evaporation of $ZnCl_2$ powder in Ar/O_2 gas flow.[13] For ZnO nanowires and nanorods, different catalysts, different temperatures, and different fabrication atmospheres were reported. Synthesis of ZnO tetrapod nanorods by oxidation of Zn powder[6] and evaporation of mixture of Zn and silica powder with Fe_2O_3 used as a catalyst were reported.[12] Fabrication by evaporation of mixture of ZnO and graphite powders,[4,8] Zn powder and Au nanoparticles,[7] ZnO powders,[5] Zn powders,[9,10] and Zn and Se powder[11] were used to obtain ZnO nanowires. The temperatures of evaporation reported in the literature varied from 450°C[9] to 1400°C.[3] The synthesis of ZnO nanostructures was reported in air,[6,8] argon flow,[3,4,9,10] mixture of argon and oxygen,[7,13] and mixture of argon, oxygen and hydrogen.[11] The obtained products were most frequently described as white (spongy or fluffy) material,[5-9] though gray color material,[4,5] yellow material,[10] and dark red material[11] were reported as well.

Optical properties of ZnO thin films and nanostructures have been extensively studied.[14-24] However, in spite of extensive studies there is no consensus in the literature on the positions and origin of the peaks in the visible emission from ZnO thin films and nanostructures. Most commonly observed feature in the visible emission of ZnO is strong and broad green emission. Typically adopted explanation for green emission in ZnO is transition between photoexcited hole and singly ionized oxygen vacancy, as proposed by Vanheusden *et al.*[14] to explain 510 nm emission. However, this explanation has been used to explain visible emission in ZnO from 495 nm[6] to 583 nm.[24] It is unlikely that there is a single transition which could explain such large variation of the center peak position for the green luminescence. Green luminescence in ZnO was

also attributed to donor-acceptor complexes,[15,16] antisite oxygen,[17] and surface states.[1,8] In addition to green luminescence, violet and blue luminescence from ZnO thin films, nanoparticles, and whiskers were reported before.[18-22] In this spectral region, the peaks at 405 nm,[21] ~420 nm,[19,20,22] 446 nm,[18] and ~485 nm[2,19] were reported. Blue luminescence at 405 nm has been attributed to zinc vacancy,[21] which is in agreement with the calculations.[17] The emission at ~420 nm has been attributed to interstitial oxygen,[2,20] transition between defects (interface traps) at grain boundaries and valence band, and lattice defects related to oxygen and zinc vacancies[19] while calculations predict 427 nm emission due to interstitial zinc.[17] The emission at 446 nm was attributed to the transition between shallow donor (oxygen vacancy) to the valence band.[18] 485 nm emission was attributed to a transition between oxygen vacancy and interstitial oxygen[2] and lattice defects related to oxygen and zinc vacancies.[19] In addition to violet, blue, and green emissions from ZnO reported in the literature, yellow emission[21] and red emission (640 nm) in ZnO thin films fabricated by spray pyrolysis was also reported.[23] The yellow emission has been assigned to interstitial oxygen[21] and oxygen vacancy (583 nm emission from tubular ZnO whiskers).[24] Calculations predict that interstitial oxygen should produce emission at ~544 nm.[17] Due to many different peak wavelengths reported, it is very likely that multiple types of defects are responsible for the visible emission in ZnO and a detailed study is necessary to conclusively identify their origin.

In this work, we investigated the influence of the growth temperature, catalyst ratio, and fabrication atmosphere to the structural and optical properties of ZnO nanostructures. Obtained nanostructures were characterized using scanning electron microscopy (SEM), transmission electron microscopy (TEM), X-ray diffraction (XRD), and room temperature photoluminescence (PL). The paper will be organized as follows. In the following section, experimental details are described. In Section 3, obtained results are presented and discussed. Finally, conclusions are drawn.

2. EXPERIMENTAL DETAILS

Zn powder (99.9 % purity from Fluka) with and without graphite powder was evaporated in a quartz tube at different temperatures. The quartz tube was inserted after the furnace has reached the desired temperature and, for Ar and N_2 flow, gas flow at rate 0.7 liter per minute was established. For deposition in humid gas flow, the gas was passed through water before being introduced into the furnace. After specified time (10-90 min. depending on deposition temperature), the quartz tube was removed from the furnace and rapidly cooled to room temperature. Comparison between different atmospheres was performed for growth temperature of 950°C and 10 min. deposition. For the same growth temperature we have investigated the influence of zinc to graphite ratio to the properties of the obtained deposition products. In all cases, except dry nitrogen flow, which yielded mixture of white and gray products, white deposition products were obtained. The structure of deposited materials was investigated by X-ray diffraction using Siemens D5000 X-ray diffractometer, scanning electron microscopy using Cambridge-440 SEM, and transmission electron microscopy using Philips Tecnai-20 TEM. The room temperature photoluminescence was measured using HeCd laser excitation source (325 nm).

3. RESULTS AND DISCUSSION

Figure 1 shows the SEM images of ZnO nanostructures obtained at 900°C, 950°C, 1000°C, and 1050°C in air. For higher deposition temperature no nanosized products were obtained, while lower temperatures there was no deposition. The deposition temperature can be lowered by using lower purity of the starting Zn material. 98% Zn can produce 99.9% purity ZnO tetrapod nanorods at deposition temperature as low as 800°C. However, since it is not clear which of the metal impurities acts as a catalyst and how metal impurities would change growth mechanism, we have chosen to study in more detail nanostructures produced from high purity Zn powder. It can be observed that 950°C is the optimal deposition temperature. At higher temperatures, more large size tetrapods as well as "clumps" can be observed. At 900°C, only tetrapods are obtained but they exhibit more broad size distribution compared to deposition at 950°C. It was found that relatively narrow temperature window for the fabrication of ZnO nanostructures exist. The temperature influences the fabrication yield and the size distribution of the tetrapod nanorods, but no other significant differences in the obtained products are obtained. We also investigated the influence of the zinc to graphite ratio to the obtained deposition products. No significant differences were found in the structure and optical properties of the obtained ZnO nanostructures with

graphite (graphite concentration range from 0.1 to 0.5) and without graphite. Similar results were also obtained if TiO_2 is used instead of graphite. Therefore, to investigate the influence of the fabrication in different atmospheres, no catalyst was used.

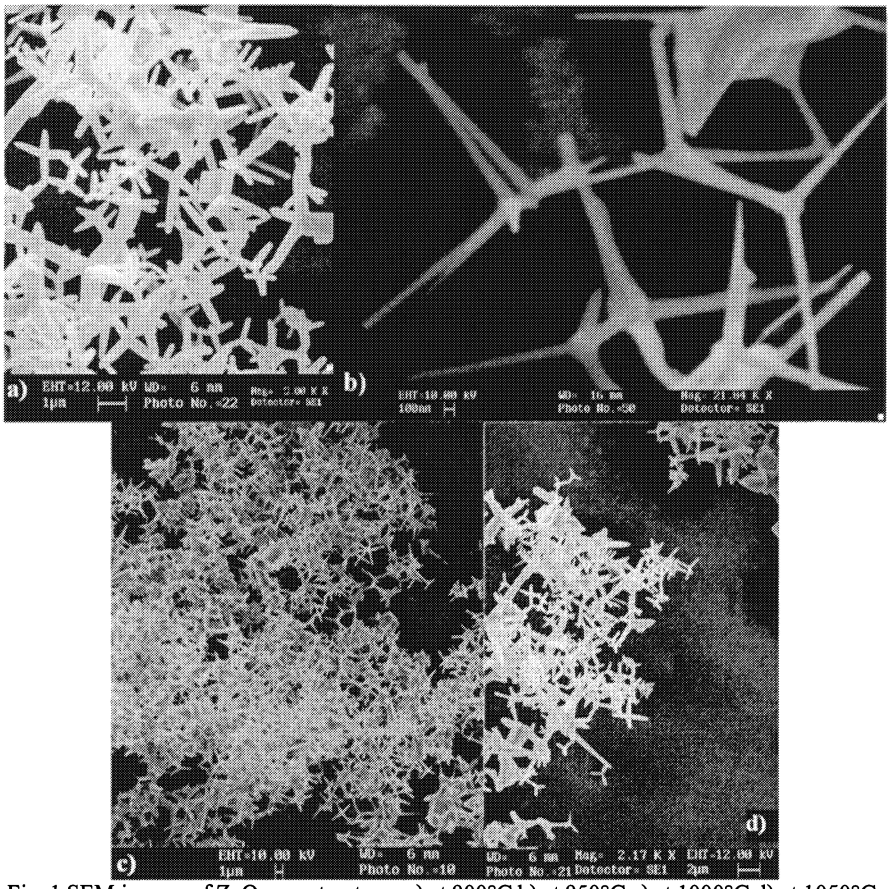

Fig. 1 SEM images of ZnO nanostructures a) at 900°C b) at 950°C c) at 1000°C d) at 1050°C.

Figure 2 shows SEM images of the obtained ZnO nanostructures in air, argon flow, humid argon flow, nitrogen flow, and humid nitrogen flow. In all cases, at higher temperature end of the quartz tube, large rods can be found, as illustrated in Fig. 2a on the right for deposition in air. In air, only tetrapod ZnO rods can be found. For deposition in air, tetrapod nanorods can be found. Observation of ZnO tetrapod nanorods is similar to the result reported by Dai *et al.*[6] and Tang *et al.*[12] who also reported synthesis of ZnO tetrapod nanorods, former in air and latter in argon flow. In the reported results in the literature, both vapor-liquid-solid[12] and vapor-solid[9] growth mechanisms were proposed for ZnO tetrapod nanorod growth. Since in our work no catalyst was used, it is likely that the growth mechanism is vapor-solid similar to the result reported by Dai *et al.*[6] Growth of the large tetrapod ZnO crystals[25,26] was studied in more details than the growth of ZnO tetrapods on submicron scale. The tetrapod growth was found to be consistent with octa-twin model.[25] Growth of large ZnO tetrapod crystals from octahedral nucleus having zincblende symmetry in initial stages of growth was proposed, and it was found that tetrapod legs are single crystal hexagonal ZnO with a [0001] growth direction.[26] However, at present is not clear whether the formation of ZnO tetrapods on submicron scale follows the same mechanism as the growth of large tetrapod crystals. Obtained XRD diffraction patterns (shown for fabrication in air in Fig. 3) show only peaks corresponding to hexagonal ZnO. No peaks from Zn or other impurities were detected. Similar results are obtained for all growth temperatures and all fabrication atmospheres. In the case of fabrication in gas flow (Fig. 2b-e), a mixture of ZnO tetrapod nanorods and nanowires is obtained. For dry argon and dry nitrogen flow, we can also identify regions where only tetrapods

are present. However, the length of tetrapod legs is significantly smaller (smaller than 1 μm) than for tetrapods obtained in air. In all cases of gas flow, we can observe mixture of tetrapods and nanowires growing out of the end of the tetrapod legs. The diameter of these nanowires is typically in the range 20-50 nm, which is significantly smaller than the tetrapod leg diameter which is typically in the range 80-150 nm. The length of the wires is in the range of several micrometers, though shorter wires in the beginning stages of growth can occasionally be found.

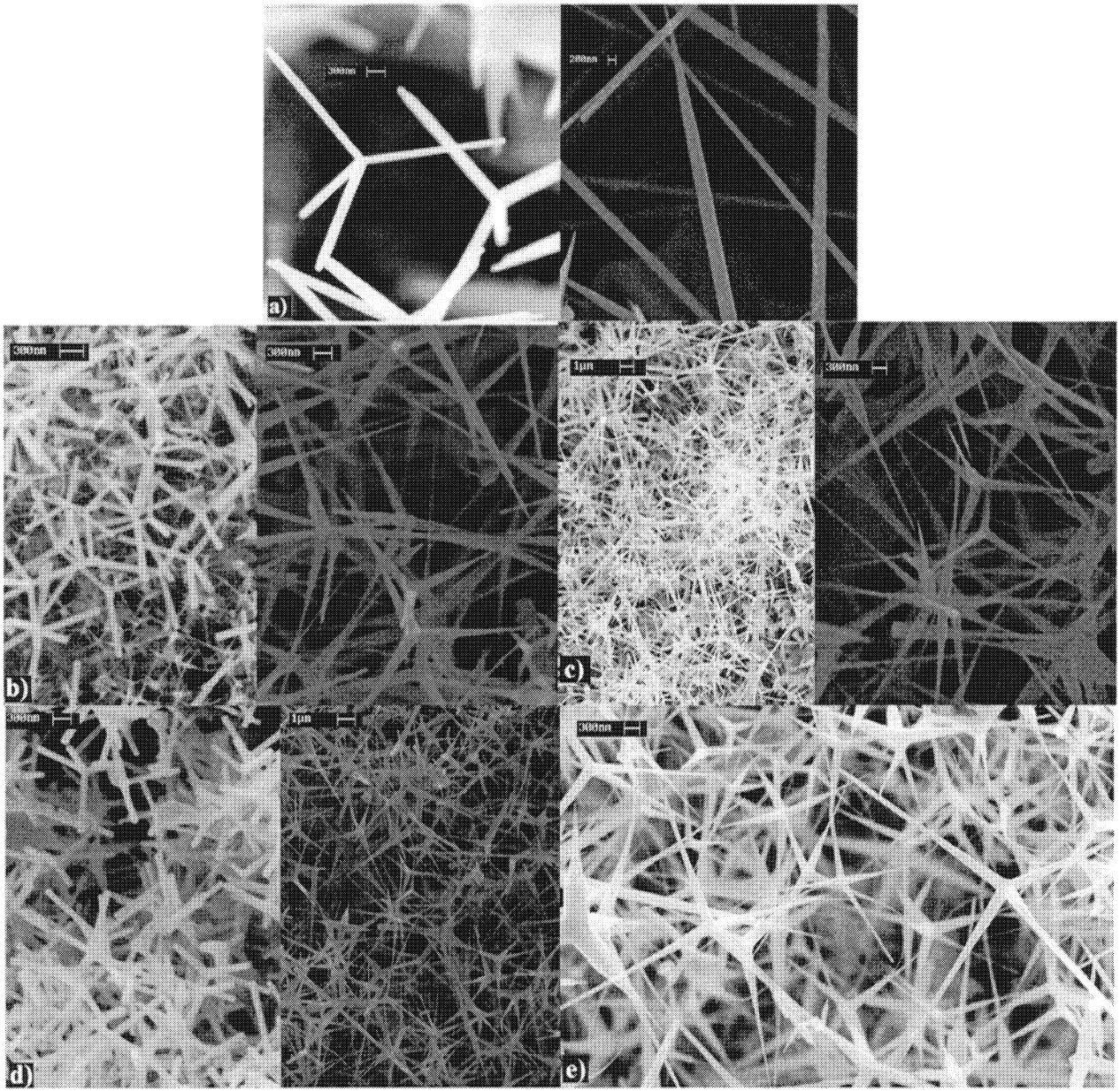

Fig. 2 SEM images of ZnO nanostructures a) in air b) in dry nitrogen flow c) in humid nitrogen flow d) in dry argon flow e) humid argon flow.

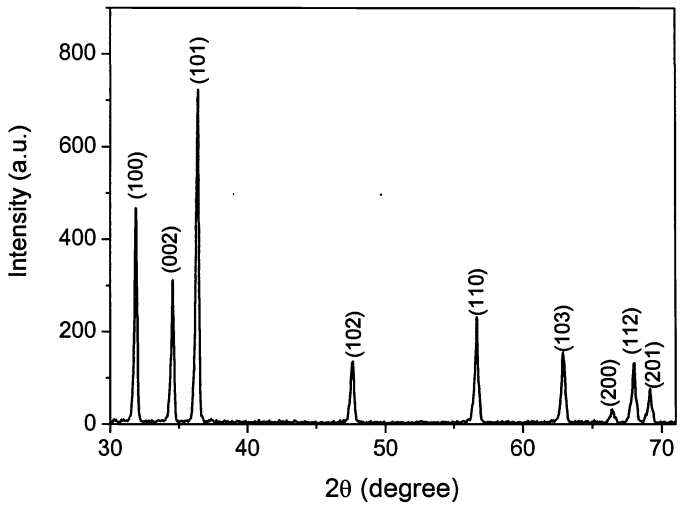

Fig. 3 XRD pattern from ZnO tetrapod nanorods deposited at 950°C in air

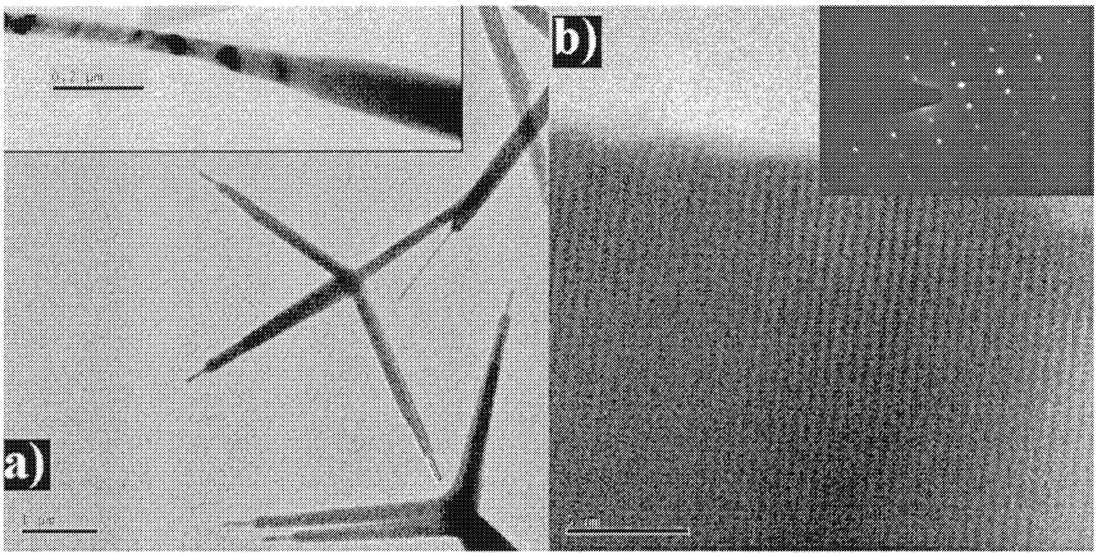

Fig. 4 TEM image of a) beginning stages of nanowire growing out of a tetrapod leg; the inset shows higher magnification image of nanowire – tetrapod leg junction. b) HR TEM of ZnO nanowire. The inset shows selected area electron diffraction pattern.

In order to study the individual structure of the obtained nanowires and nanorods, TEM, high resolution TEM and selected area electron diffraction (SAED) were performed. Figure 4a shows the beginning stages of the nanowire growth from the tetrapod leg. The inset shows enlarged tetrapod leg-nanowire junction. The junction region is typically showing ripple-like contrast, which is most likely due to strain. The ripples are more pronounced with bending of the nanowires growing out of the tetrapod. Fig. 4b shows the high resolution TEM image with clear lattice fringes indicating single crystalline structure, while the inset shows selected area electron diffraction pattern. For some nanowires, very thin amorphous layer can be observed at the edge, which is similar to the result reported by Yao *et al.*[8] From the obtained results

and the spacing between two adjacent lattice plains (~2.6 Å), it can be concluded that the wires grow along [0001] direction. This is in agreement with previous reports on the growth of ZnO nanowires, which also reported growth along [0001] direction.[4,8] At present, it is not fully clear why growth of ZnO nanowires from the end of the tetrapod legs is observed. More detailed study of the growth mechanisms and nanowire nucleation sites is necessary in order to draw any definite conclusions on the observed phenomenon. However, based on the analogy with the growth of GaN nanowires in absence of catalyst, it is possible that the growth is controlled by oxygen atom supply. For the growth of GaN nanowires from the sides of hexagonal GaN crystal platelets, it was found that the growth of GaN nanowires from the side of the platelets was mainly due to platelet growth being limited by the N atom supply.[27] In this work, oxidation of Zn in inert gas flow and thus more limited oxygen availability compared to oxidation in air resulted in growth of nanowires from the end of tetrapods. For the deposition in air, no nanowire growth was observed.

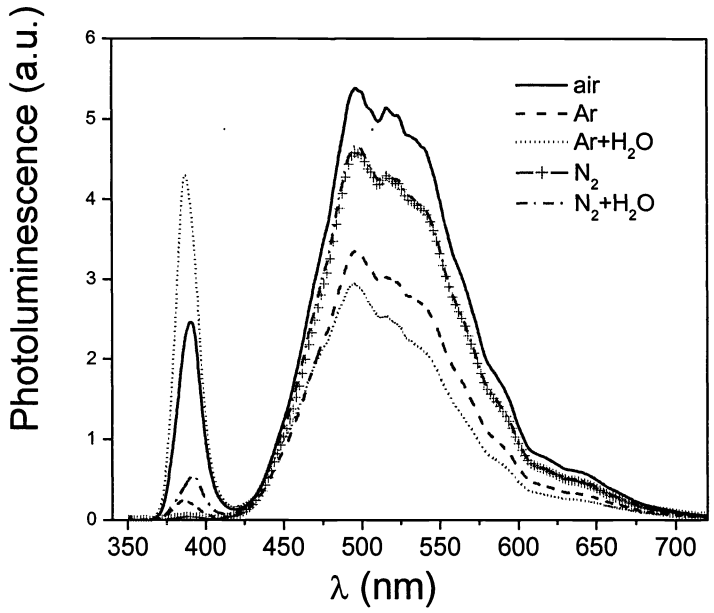

Fig. 5 Photoluminescence of ZnO nanostructures prepared in different atmospheres.

Figure 5 shows photoluminescence spectrum of ZnO nanostructures prepared in different atmospheres. It can be observed that the gas flow has significant influence on the ratio of UV to visible emission. In the visible spectral range, two main peaks ~495 nm and ~520 nm can be identified, which is in good agreement with the PL of ZnO nanowires reported by Park *et al.*[6] Previous study of ZnO tetrapod nanorods reported broad visible emission at 495 nm.[6] Since the emission in the visible spectral region in Zn oxide is related to various structural defects, UV to visible emission ratio is a good indicator of the quality of obtained material. Only nanostructures deposited in air and humid argon flow exhibit significant UV emission. In all cases except humid argon flow, green emission is more intense than the UV emission. The UV emission is entirely absent for sample fabricated in dry nitrogen flow, while samples in dry argon and humid nitrogen flow show weak UV and strong green emission. At present it is not fully clear why are such differences obtained. For the fabrication in nitrogen flow, possible cause of UV emission suppression may be nitrogen doping. It is known that nitrogen acts as acceptor in ZnO.[28] Also, calculations indicate that hydrogen can act as a shallow donor,[29] which may contribute to the differences between the samples fabricated in dry and humid gas flow. It was reported previously that the ratio of UV to green emission is dependent on the nanostructure sizes.[4] However, we were not able to observe any significant relationship between the size

of the obtained nanostructures and the green emission. The highest UV to visible emission intensity ratio was obtained for the fabrication in humid argon flow which produces, on average, smaller structures than fabrication in air.

4. CONCLUSION

In conclusion, we have fabricated ZnO tetrapod nanorods and nanowires using a simple method. The influence of the temperature, catalyst, and fabrication atmosphere on the morphology and optical properties of the obtained nanostructures was investigated. Temperature was found to influence the yield and the size of structures obtained, while it didn't change the morphology. It was found that the fabrication in air results in tetrapod nanorods, while for gas flow mixture of tetrapod nanorods and nanowires is obtained. The difference in the obtained morphologies with and without gas flow was attributed to the availability of oxygen atoms. Limited oxygen supply results in nanowire growth from the end of the tetrapod. Different fabrication atmosphere also had significant influence on the ratio of UV to visible emission. The highest UV to visible ratio was obtained for fabrication in humid argon flow.

ACKNOWLEDGEMENTS

The authors would like to thank Amy Wong and Wing Sang Lee for SEM and TEM measurements and Dr. M. H. Xie for useful discussions.

REFERENCES

1. S. Monticone, R. Tufeu, and A. V. Kanaev, "Complex nature of the UV and visible fluorescence of colloidal ZnO nanoparticles", J. Phys. Chem. B **102**, pp. 2854-2862, April 1998.
2. S. Mahamuni, K. Borgohain, B. S. Bendre, V. J. Leppert, and S. H. Risbud, "Spectroscopic and structural characterization of electrochemically grown ZnO quantum dots", J. Appl. Phys. **85**, pp. 2861-2865, March 1999.
3. Z. W. Pan, Z. R. Dai, and Z. L. Wang, "Nanobelts of semiconducting oxides", Science **291**, pp. 1947-1949, March 2001.
4. M. H. Huang, Y. Wu, H. Feick, N. Tran, E. Weber, and P. Yang, "Catalytic Growth of Zinc Oxide Nanowires by Vapor Transport", Adv. Mater. **13**, pp. 113-116, Jan. 2001.
5. K. Park, J. S. Lee, M. Y. Sung, and S. Kim, "Structural and Optical Properties of ZnO Nanowires Synthesized from Ball-Milled ZnO Powders", Jpn. J. Appl. Phys. **41**, pp. 7317-7321, Dec. 2002.
6. Y. Dai, Y. Zhang, Q. K. Li, and C. W. Nan, "Synthesis and optical properties of tetrapod-like zinc oxide nanorods", Chem. Phys. Lett. **358**, pp. 83-86, May 2002.
7. Y. W. Wang, L. D. Zhang, G. Z. Wang, X. S. Peng, Z. Q. Chu, and C. H. Liang, "Catalytic growth of semiconducting zinc oxide nanowires and their photoluminescence properties", J. Crystal Growth **234**, pp. 171-175, Jan. 2002.
8. B. D. Yao, Y. F. Chan, and N. Wang, "Formation of ZnO nanostructures by a simple way of thermal evaporation", Appl. Phys. Lett. **81**, pp. 757-759, July 2002.
9. S. C. Lyu, Y. Zhang, H. Ruh, H. J. Lee, H. W. Shim, E. K. Suh, and C. J. Lee, "Low temperature growth and photoluminescence of well-aligned zinc oxide nanowires", Chem. Phys. Lett. **363**, pp. 134-138, Sept. 2002.
10. J. Y. Li, X. L. Chen, H. Li, M. He, and Z. Y. Qiao, "Fabrication of zinc oxide nanorods", J. Crystal Growth **233**, pp. 5-7, Nov. 2001.
11. Y. C. Kong, D. P. Yu, B. Zhong, W. Fang, and S. Q. Feng, "Ultraviolet-emitting ZnO nanowires synthesized by a physical vapor deposition approach", Appl. Phys. Lett. **78**, pp. 407-409, 2001.
12. C. C. Tang, S. S. Fan, M. L. de la Chapelle, and P. Li, "Silica-assisted catalytic growth of oxide and nitride nanowires", Chem. Phys. Lett. **333**, pp. 12-15, Jan. 2001.
13. J. Zhang, W. Yu, and L. Zhang, "Fabrication of semiconducting ZnO nanobelts using a halide source and their photoluminescence properties", Phys. Lett. A **299**, pp. 276-281, July 2002.
14. K. Vanheusden, W. L. Warren, C. H. Seager, D. R. Tallant, J. A. Voigt, and B. E. Gnade, "Mechanisms behind green photoluminescence in ZnO phosphor powders", J. Appl. Phys. **79**, pp. 7983-7990, May 1996.

15. S. A. Studenikin and M. Cocivera, "Time-resolved luminescence and photoconductivity of polycrystalline ZnO films", J. Appl. Phys. **91**, pp. 5060-5065, April 2002.
16. D. C. Reynolds, D. C. Look, and B. Jogai, "Fine structure on the green band in ZnO", J. Appl. Phys. **89**, pp. 6189-6191, June 2001.
17. B. Lin, Z. Fu and Y. Jia, "Green luminescent center in undoped zinc oxide films deposited on silicon substrates", Appl. Phys. Lett. **79**, pp. 943-945, Aug. 2001.
18. Z. Y. Xue, D. H. Zhang, Q. P. Wang, and J. H. Wang, "The blue photoluminescence emitted from ZnO films deposited on glass substrate by rf magnetron sputtering", Appl. Surf. Sci. **195**, pp. 126-129, July 2002.
19. J. Q. Hu, X. L. Ma, Z. Y. Xie, N. B. Wong, C. S. Lee, and S. T. Lee, "Characterization of zinc oxide crystal whiskers grown by thermal evaporation", Chem. Phys. Lett. **344**, pp. 97-100, Aug. 2001.
20. X. L. Xu, S. P. Lau, J. S. Chen, G. Y. Chen, and B. K. Tay, "Polycrystalline ZnO thin films on Si (100) deposited by filtered cathodic vacuum arc", J. Crystal Growth **223**, pp. 201-205, Feb. 2001.
21. X. L. Wu, G. G. Siu, C. L. Fu, and H. C. Ong, "Photoluminescence and cathodoluminescence studies of stoichiometric and oxygen-deficient ZnO films", Appl. Phys. Lett. **78**, pp. 2285-2287, April 2001.
22. B. J. Jin, S. Im, and S. Y. Lee, "Violet and UV luminescence emitted from ZnO thin films grown on sapphire by pulsed laser deposition", Thin Solid Films **366**, pp. 107-110, May 2000.
23. S. A. Studenikin, N. Golego, and M. Cocivera, "Fabrication of green and orange photoluminescent, undoped ZnO films using spray pyrolysis", J. Appl. Phys. **84**, pp. 2287-2294, Aug. 1998.
24. J. W. Hu and Y. Bando, "Growth and optical properties of single-crystal tubular ZnO whiskers", Appl. Phys. Lett. **82**, pp. 1401-1403, March 2003.
25. H. Iwanaga, M. Fujii, M. Ichihara, and S. Takeuchi, "Some evidence for the octa-twin model of tetrapod ZnO particles", J. Crystal Growth **141**, pp. 234-238, Aug. 1994.
26. M. Kitano, T. Hanabe, S. Maeda, and T. Okabe, "Growth of large tetrapod-like ZnO crystals. II. Morphological considerations on growth mechanism", J. Crystal Growth **108**, pp. 277-284, Jan. 1991.
27. M. He, P. Zhou, S. Noor Mohammad, G. L. Harris, J. B. Halpern, R. Jacobs, W. L. Sarney, and L. Salamanca-Riba, J. "Growth of GaN nanowires by direct reaction of Ga with NH_3", Crystal Growth **231**, pp. 357-365, Oct. 2001.
28. A. B. M. Almamun Ashrafi, I. Suemune, H. Kumano, and S. Tanaka, "Nitrogen-doped p-type ZnO layers prepared with H_2O vapor-assisted metalorganic molecular-beam epitaxy", Jpn. J. Appl. Phys. Part 2 Letters, **41**, pp. L1281-1284, Nov. 2002.
29. C. G. Van de Walle, "Hydrogen as a cause of doping in zinc oxide", Phys. Rev. Lett. **85**, pp. 1012-1015, July 2000.